Proceedings of the
Annual Stability Conference
Structural Stability Research Council
Orlando, Florida, April 13-15, 2016

An Introspective Assessment of Buckling and Second-Order Load-Deflection Analysis Based Design Calculations

Woo Yong Jeong[1], Oğuzhan Toğay[2], Ajinkya M. Lokhande[3], Donald W. White[4]

Abstract
SSRC Technical Memorandum No.5 states that the nominal design resistance of structural steel members and frames generally should be taken as the maximum resistance of the geometrically imperfect structure containing initial residual stresses. In Specification member resistance equations, this requirement is satisfied commonly as a "mapping" from the theoretical member buckling load. That is, the engineer calculates the theoretical buckling load and the design resistance equations then convert this ideal buckling strength to the nominal member resistance for the corresponding strength limit state. These mappings are often tied to concepts of tangent stiffness and its influence on buckling and/or concepts of reaching a maximum cross-section resistance of some type in the member containing initial geometric imperfections. In recent research, various attempts have been made to develop design procedures based on direct modeling, in the structural analysis, of all geometric imperfections that have a significant impact on the structural resistance. In addition, inelastic buckling analysis based procedures have been developed that provide for a fast and more rigorous computational assessment of member inelasticity, end restraint from continuity across braced points, moment gradient, and load height effects. These procedures do not require the modeling of member imperfections (e.g., out-of-straightness and initial twist) in the structural analysis.

This paper compares the procedures and the results using these different approaches and discusses their respective strengths and limitations for an adaptation of a roof girder design example originally developed by the AISC Ad hoc Committee on Stability Bracing (AISC 2002)

1. Introduction
Traditional design methods, such as the Effective Length Method (the ELM) and the Direct Analysis Method (DM), are widely employed to evaluate the required design strength of structural steel members and frames. In these methods, a second-order elastic load-deflection analysis is performed to estimate member internal forces. In addition, the member resistance is calculated by separately determining various design strength factors, such as the member effective length factor,

[1] Research Associate, Georgia Institute of Technology, <wyjeong77@gmail.com >
[2] Graduate Research Assistant, Georgia Institute of Technology, <oguzhantogay@gatech.edu>
[3] Graduate Research Assistant, Georgia Institute of Technology, <alokhande3@gatech.edu>
[4] Professor, Georgia Institute of Technology, <don.white@gatech.edu>

K, and moment gradient and load height modifiers, C_b. Designs are evaluated by comparing the required strength obtained from the analysis to the member resistance.

The selection of an unbraced length for the calculation of the flexural resistance is based typically on the assumption of full bracing. The accurate calculation of the moment gradient and load height modifier, C_b under general conditions, such as moment gradient load, load height, and different types of end restraint is still illusive. Thus, the calculation of member resistance results in inaccuracy under general loadings, general end conditions, and general intermediate conditions.

For advanced design of steel members and frames, AISC (2016) Appendix 1.2 and 1.3 are presented. The design evaluation using Appendix 1.2 and 1.3 is performed by directly modeling initial geometric imperfections. By appropriate modeling of potential member geometric imperfections, a second-order elastic load-deflection analysis can capture a critical failure mode(s) of the member and/or frame. However, the available strength in Appendix 1.2 requires the manual calculation of the member nominal flexural strength for a specified unbraced length, since the design by Appendix 1.2 is based on elastic analysis. The available strength may be obtained using Appendix 1.3 but there are numerous modeling complexities, some requiring significant understanding and interpretation of the underlying behavior.

There is generally some loss of rigor associated with combining a second-order elastic load-deflection analysis with the traditional application of separate manual strength equations. White et al. (2015) presents a comprehensive approach for the design of structural steel members and frames via the use of buckling analysis combined with appropriate column, beam and beam-column inelastic stiffness reduction factors. The stiffness reduction factors are derived from the ANSI/AISC 360 Specification column, beam and beam-column strength provisions. This approach can be employed to account for column, beam, and beam-column strength considering general loadings, general end conditions, and general intermediate conditions. Furthermore, the approach can be extended to member and stability bracing design of beams and beam-columns. This paper introduces the use of the structural analysis software, SABRE2 (White et al. 2016), which incorporates the AISC member strength equations ubiquitously within a buckling analysis, via calculated net stiffness reduction factors (SRFs), to provide a more rigorous characterization of the member resistances.

The paper first presents the problem statement for an example roof girder and its bracing system. The example is adapted from a prior case study developed by the AISC Ad hoc Committee on Stability Bracing (AISC 2002). Then, the evaluation of this member and its bracing system using the various methods defined within the AISC (2016) Specification – the ELM, the DM, Appendix 1.2, Appendix 1.3, and inelastic buckling analysis is considered. The advantages and limitations for each method are studied.

2. Problem Description

To assess and discuss required strength and bracing stiffness using different approaches in the AISC Specification, an adaptation of a roof girder design example developed by the AISC Ad hoc committee on Stability Bracing (AISC 2002) is studied. The structure is illustrated in Fig.1.

The girder has a 70 ft span and is subjected to gravity loading applied from outset roof purlins connected to its top flange and spaced at 5 ft on center. The purlins are assumed to span 25 ft between the roof girders in the out-of-plane direction and are taken as continuous over the girder locations. End negative moments are transmitted to the girders due to the rotational restraint from the columns in a clear span portal frame that this member is a component of, and end axial compression loads are applied to the girder due to the thrusts at the foundation level. The girder is considered as a subassembly isolated from the rest of the frame in this example. Consistent with common practice, the ends of the subassembly are assumed to be flexurally and torsionally simply supported. That is, the girder flanges are assumed to be free to rotate about the axis of the web (i.e., both the warping and out-of-plane lateral bending of the flanges is unrestrained at the girder ends), and the girder major-axis bending rotations are assumed to be unrestrained at the member ends. The vertical and out-of-plane lateral deflections and the twist rotations at the ends of the girder are assumed to be rigidly restrained at these positions.

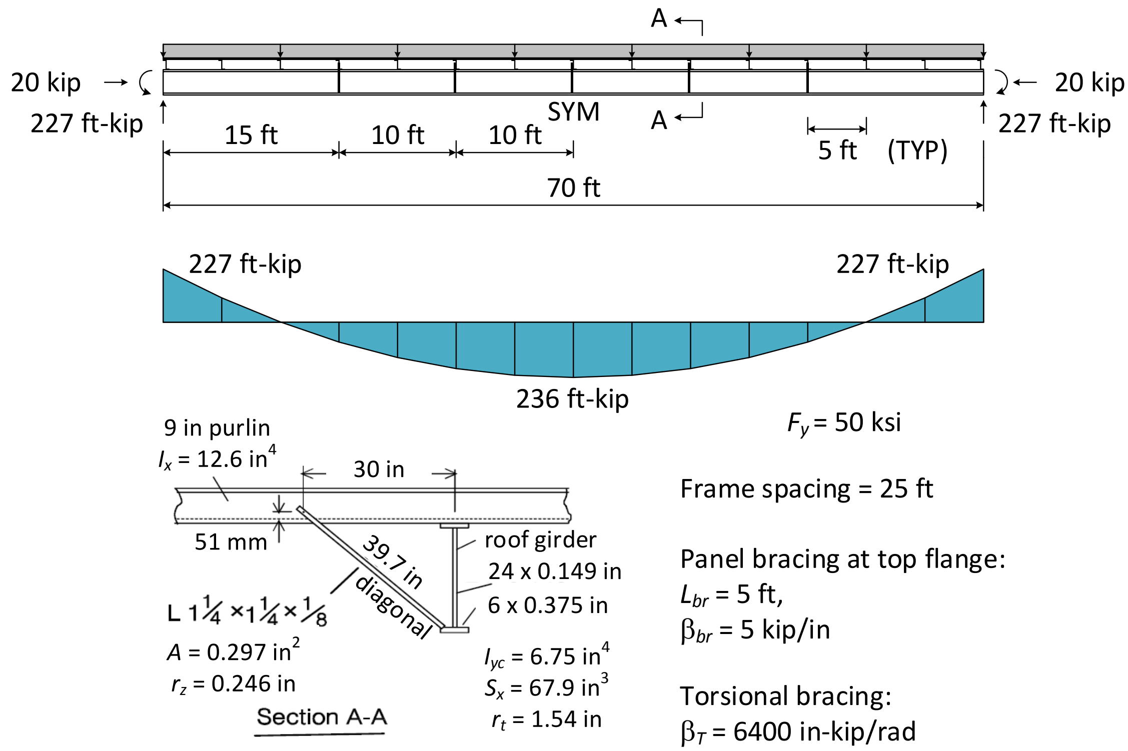

Figure 1. Roof girder example, adapted from (AISC 2002).

The top flange in this problem is assumed to be braced at the purlin locations by light-weight roof deck panels, having a shear panel stiffness of 5 kip/in (G' = 1 kip/in) and having a shear strength of 125 plf. Flange diagonal braces are provided from the purlins to the bottom flange at the mid-span of the girder plus at two additional locations on each side of the mid-span with a spacing of 10 ft between each of these positions. These diagonal braces restrain the lateral movement of the bottom flange relative to the top flange, and therefore they are classified as torsional braces. The provided elastic torsional bracing stiffness from the combination of these components and the roof purlins is taken as β_T = 6400 in-kip/rad. This estimate of the provided torsional bracing stiffness is outlined in (AISC 2002). These torsional braces combine with the panel lateral bracing from the roof deck to provide out-of-plane lateral stability to the roof girder.

The above bracing stiffnesses are divided by 2/ϕ and the corresponding reduced stiffnesses are employed for inelastic buckling analysis, per AISC Appendix 6 (AISC 2016). That is, given the calculation of the ideal bracing stiffnesses β_i, i.e., the bracing stiffness necessary to develop the required load in a buckling analysis model, the design philosophy of AISC Appendix 6 is that the required stability bracing stiffnesses are 2/ϕ times the β_i values. This practice is derived from Winter (1960), who showed that in general, bracing stiffnesses larger than β_i are necessary to avoid excessive second-order amplification of the bracing system deformations and internal forces. When the nominal bracing stiffnesses are specified as in the above, they are divided by 2/ϕ to allow for an inelastic buckling analysis assessment consistent with this practice.

The AISC (2002) calculations are based on the assumption that the roof diaphragm is effectively rigid. In addition, the axial compression in the roof girder is assumed to be zero in the original calculations. Given the above adaptations to include flexible panel bracing and girder axial force, there are multiple attributes of this example that present substantial unknowns and/or difficulties for assessment of the roof girder by traditional methods:

1) If the panel bracing system required stiffness is checked just for the demands from the flexural loading using the base AISC (2016) Appendix 6 rules, i.e.,

$$\beta_{br} = \frac{2}{\phi}\frac{(M_{u.\max}/h_o)\,C_d C_t}{L_{br}} = \frac{2}{0.75}\frac{(236\text{ ft-kip}/24.375\text{ in})\;x\;1\;x\;2}{5\text{ ft}} = 10.3\,\frac{\text{kip}}{\text{in}}$$

   one can conclude that the panel bracing system does not provide full bracing. This does not preclude the consideration of partial bracing from the roof panels, but such considerations are beyond the scope of Appendix 6.
2) The roof girder is braced out-of-plane by a combination of panel bracing at it top flange and torsional bracing from the purlins and flange diagonal braces at selected locations. In addition, the roof girder is subjected to combined axial compression and major-axis bending. AISC (2016) Appendix 6 does not provide direct guidance for assessment of combined bracing systems and/or general bracing of beam-column members, other than generally permitting buckling analysis methods such as in SABRE2 (White et al. 2016) for assessment of the bracing stiffness. Some new guidance regarding these considerations is provided in the AISC (2016) Appendix 6 Commentary.
3) The torsional braces are not uniformly spaced along the length of the roof girder. The torsional brace spacing is 15 ft at the girder ends in the above design, and 10 ft in the four interior segments. The Appendix 6 torsional bracing rules are based on an underlying model involving lateral torsional buckling of an elastic I-section member braced by continuous torsional bracing, and the application of this model to discrete torsional bracing by effectively summing the torsional bracing stiffnesses and dividing by the total member length. It is anticipated that this approximation is slightly conservative in the maximum positive moment region of the above roof girder and slightly optimistic in the negative moment regions at the girder ends. However, the specific magnitudes of the approximation are unknown.

Therefore, this is a good example to consider challenges encountered in the different AISC design approaches and to evaluate a practical inelastic buckling approach based on the AISC Specification provisions. In the following sections, various approaches are studied to evaluate the above girder design resistance as well as the adequacy of its bracing system.

3. Assessment by the Effective Length and Direct Analysis Methods

For the routine design of typical steel members or frames, the AISC Direct Analysis Method (the DM) or the Effective Length Method (the ELM) may be employed.

For a calculation of required design strength using the DM and the ELM, a second-order elastic analysis is required and calculation of available strength of members and connections is conducted in accordance with the AISC Chapters D, E, F, G, H, I, J and K as applicable. A column inelastic effective length factor K is required generally ($K \leq 1$ in the DM) to determine the most accurate estimate of the nominal compressive strength of members, P_n, based on the Specification equations. Similarly, an inelastic lateral-torsional buckling effective length factor, K, and a lateral-torsional buckling modification factor, C_b, for moment gradient loading and load height is required generally to determine the most accurate estimate of the nominal flexural strength of members, M_n.

To calculate the required strengths using the ELM, the second-order elastic analysis is performed with the following required considerations:

1) All loads correspond to LRFD load combinations or 1.6 times the ASD load combinations.
2) All significant member deformations.
3) Second-order effects (both $P\text{-}\Delta$ and $P\text{-}\delta$ effects).
4) Geometric imperfections using notional loads.
5) No Stiffness reduction.
6) Calculated effective length factor K.

To calculate required strengths using the DM, the second-order elastic analysis is performed with the following required considerations:

1) All loads correspond to the LRFD load combinations or 1.6 times the ASD load combinations.
2) All significant member deformations.
3) Second-order effects (both $P\text{-}\Delta$ and $P\text{-}\delta$ effects).
4) Geometric imperfections using direct modeling or notional loads.
5) Stiffness reduction using $0.8\tau_a$ times the nominal elastic flexural stiffness and 0.8 times other nominal elastic stiffness.
6) Effective length factor K=1.

The DM and ELM assume that the bracing stiffness and strength are sufficient to control member movement at the bracing locations. Since the above girder qualifies as being only partially braced by the roof panels per AISC Appendix 6, at least for the internal moments at the mid-span of the girder, the specific unbraced lengths KL_y and KL_b that should be employed in the traditional calculation of the member axial and flexural resistances $\phi_c P_n$ and $\phi_b M_n$ are not easily determined. This issue precludes the use of either the Effective Length Method (ELM) or the Direct Analysis Method (DM) provisions of the AISC Specification to assess the above problem.

4. Assessment by AISC (2016) Appendix 1, Section 1.2 (Design by Elastic Analysis)

For a calculation of required design strength in Appendix 1.2, a second-order elastic analysis by directly modelling all significant member and frame imperfections is conducted. The calculation of the available strength of members and connections is conducted in accordance with the AISC (2016) Specification Chapters D, E, F, G, H, I, J and K. Using these provisions, the nominal compressive strength of members, P_n, can be calculated from the cross-section compressive strength F_yA_e where F_y is a yield strength and A_e is an effective area as defined in AISC (2016) Specification Section E-7. However, the calculation of the nominal flexural strength of members M_n still requires the definition of an unbraced length, L_b, or a lateral torsional buckling effective KL_b. In addition, the factor C_b must be determined considering the moment gradient loading and load height.

To calculate required strengths in the Appendix 1.2, the second-order elastic analysis is performed including the following required considerations:

1) All loads corresponding to LRFD load combination.
2) Torsional member deformations.
3) Geometric nonlinearities including both P-Δ and P-δ effects and twisting effects. The use of the approximate methods appearing in Appendix 8 is not permitted.
4) In all cases, direct modelling of initial imperfections, such as initial out-of-straightness (L_b/1000 or L_b/2000) between braced points and initial out-of-alignment (L_b/500) at bracing locations. The pattern of the initial imperfections is to be taken considering the greatest destabilizing effect for the load combination being considered. The use of notional loads to represent these imperfections is not permitted.
5) Stiffness reduction using $0.8\tau_a$ times the nominal elastic flexural stiffness and 0.8 times other nominal elastic stiffness.
6) The method is restricted to doubly symmetric members.

To evaluate the required strength and bracing stiffness by AISC (2016) Appendix 1.2, the roof girder is modeled using Mastan (Ziemian 2015). This model has the following characteristics:

- The 70 ft long roof girder is modeled using open-section thin-walled beam element including the contribution of cross-section warping to the element torsional stiffness. Four elements are used to represent each 5 ft long segment between the purlins in the model. These elements are assigned the following cross-section properties: A = 8.076in^2 (cross-section area), I_z = 840.1in^4 (major-axis bending moment of inertia), I_y = 13.51in^4 (minor-axis bending moment of inertia), J = 0.0001in^4 (St. Venant torsional constant, modeled as a very small value effectively equal to zero, since the web of the roof girder is slender and AISC neglects the St. Venant torsion constant in calculating the flexural resistance for slender members), and C_w = 2005 in^6 (cross-section torsional warping constant). The elastic material stiffness of the roof girder elements is modeled as 0.8x29,000ksi = 23,200ksi.

- The roof diaphragm is modeled as a shear flexible beam, which has effectively rigid properties except for its shear area. The shear area of these beams is calculated as

$$A_s = \frac{G's}{G}\phi = \frac{1\text{kip / in } x \text{ } 25\text{ft } x \text{ } 12\text{in / ft}}{11{,}150\text{ksi}} 0.8 = 0.0125\,\text{in}^2$$

where G' is the specified shear stiffness of the diaphragm, s is the diaphragm width tributary to the roof girder, equal to the spacing between the roof girders along the building length, G is the nominal elastic shear modulus of the diaphragm (the design elastic stiffness reduction is handled through ϕ=0.8).

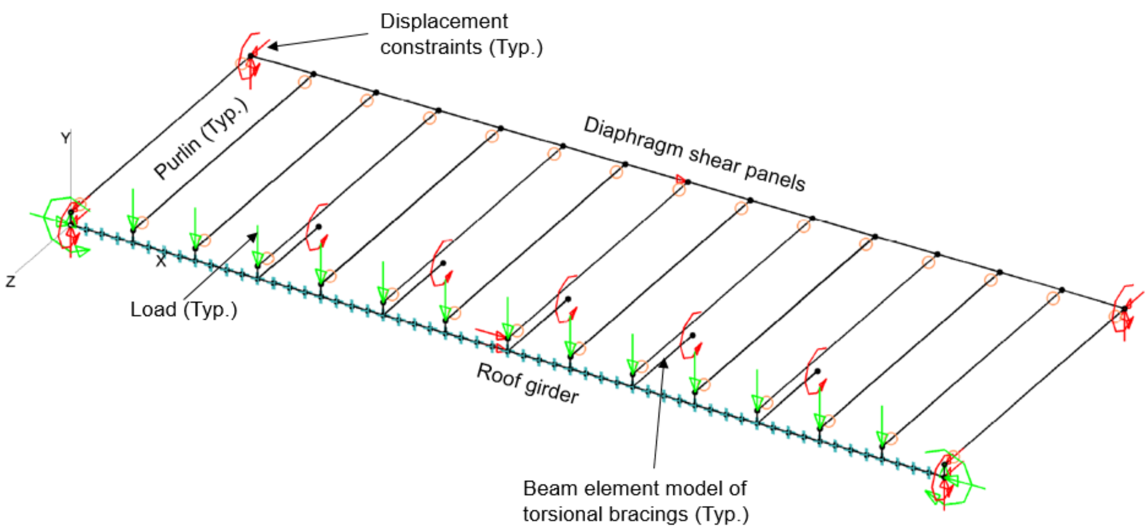

Figure 2. Matrix structural analysis model in Mastan (Ziemian 2015).

- The purlins are idealized as rigid pin-ended axial struts tying the top flange of the roof girder back to the diaphragm shear panels at 5 ft intervals along the span length. These struts are modeled such that they do not provide any contribution from their torsional stiffness to the overall structural analysis model.

- The models of the purlins and the diaphragm shear panels are created at the elevation of the top flange of the roof girder, i.e., at $h_o/2$=12.1875in above the centerline of the roof girder elements. The struts modeling the purlins are tied to the roof girders effectively by rigid struts extending from the roof girder element centroidal axis up to this elevation.

- The gravity loads are applied at the above top flange location of the roof girder elements.

- The torsional bracing spring associated with Appendix 6 and the design analysis model of Fig.2 is modeled in Mastan using 100in long beam elements having an elastic modulus of 100ksi, connected to the centroid of the roof girder elements at each of the torsional bracing locations. The rotation about the global X axis is constrained at the opposite end of these elements from the end that is connected to the roof girder. As such, these elements provide a rotational stiffness of

$$\beta_T = \frac{E_T I_T}{L_T} = I_T$$

that restraints the twisting of the roof girders where these elements are connected, where E_T=100ksi and L_T=100in are the elastic modulus and length of the beam elements representing the torsional braces, and I_T is the corresponding moment of inertia of these elements about the axis of bending corresponding to torsional rotation of the roof girders.

- The purlins and flange diagonal braces are attached to the top and bottom flanges of the roof girders in this example; therefore, as specified in Section 6.2a of the recommended Appendix 6 provisions, the effective torsional bracing stiffness does not need to be reduced to account for the distortional flexibility of the roof girders.

- The roof girder is modeled with initial geometric imperfections. Out-of-straightness of L_b/1000 or L_b/2000 and braced point out-of-alignment L_b/500 are considered in the top compression flange at the critical unbraced lengths, which are adjacent to the mid-span. The fact that these are the critical unbraced lengths is determined with the help of SABRE2 (White et al. 2016). Two types of geometric imperfections are studied, one to evaluate the torsional bracing strength requirements in addition to evaluating the girder strength (Fig.3) and one to evaluate the shear panel strength requirements in addition to evaluating the girder strength (Fig.4).

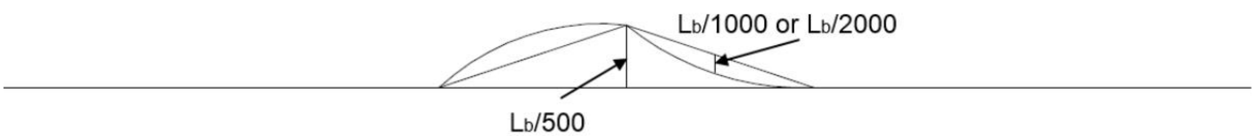

Figure 3. Out-of-straightness and braced point out-of-alignment initial geometric imperfections considered on the top flange of the roof girder to evaluate the girder strength and the torsional bracing strength requirements.

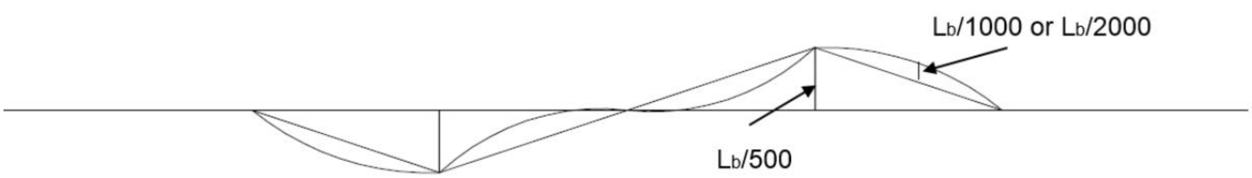

Figure 4. Out-of-straightness and braced point out-of-alignment initial geometric imperfections considered on the top flange of the roof girder to evaluate the girder strength and the shear panel bracing strength requirements.

- Lastly, the displacement constraints in the above overall structural analysis model, other than those corresponding to the beam element modeling of the torsional bracing springs, are shown in Fig.2 and may be listed as follows:
  - The left- and right-hand roof girder and diaphragm "shear beam" ends in the view shown in Fig.2. are rigidly constrained against translation in the Y, and Z directions, and they are rigidly constrained against twist about the global X axis.
  - The mid-span of the roof girder and diaphragm are rigidly constrained against translation in X direction.

After performing a second-order elastic analysis of the above model in Mastan, the deflected shape of the bracing system at an applied load ratio equal to 1 (corresponding to full application of the required design load) is shown in Fig.5 and Fig.6. The undeflected initial geometry and deformed shape of the shear panels are described in the figures. One can observe that there is lateral deformation of the diaphragm (modeled at the level of the roof girder top flange).

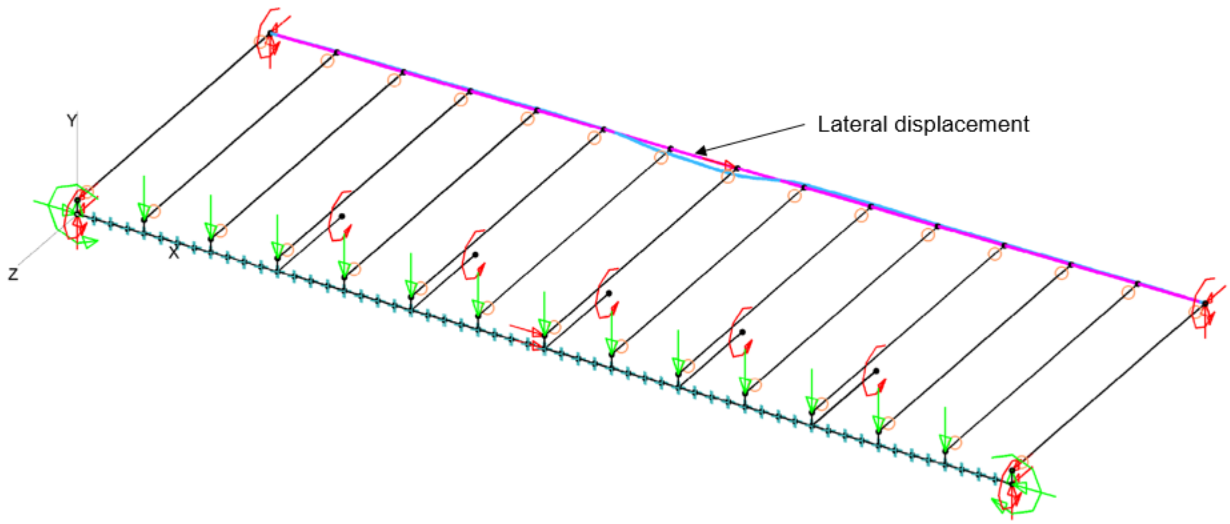

Figure 5. Second-order elastic deflected shape including imperfection in Fig.3.

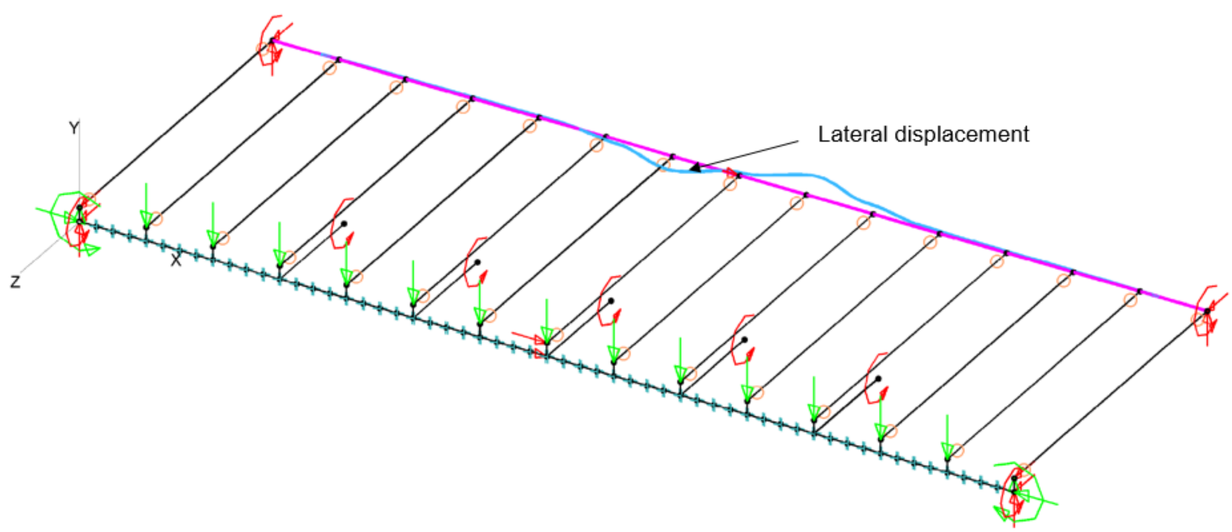

Figure 6. Second-order elastic deflected shape including imperfection in Fig.4.

The flexural nominal strength, M_n, of the partially braced roof girder is difficult to determine. Thus, the overall design strength check is difficult.

The maximum brace strength requirement for the critical torsional brace located at the mid-span of the roof girder is calculated from the second-order elastic analysis including the imperfection in Fig.3 and this requirement is:

$$\frac{\phi\beta\Delta_T}{(M_{u.\max}/h_o)}*100(\%)=\frac{0.8\ x\ 10.77\ \text{kip/in}\ x\ 0.08\ \text{in}}{(3014\ \text{in-kip}/24.375\ \text{in})}x\ 100(\%)=0.56(\%)$$

The maximum brace strength requirement for the critical shear panel bracing on each side of the mid-span is calculated from the second-order elastic analysis including imperfection in Fig.4 and this requirement is:

$$\frac{\phi\beta\Delta_{sp}}{(M_{u.\max}/h_o)}=\frac{0.8\ x\ 5\ \text{kip/in}\ x\ 0.17\ \text{in}}{(3014\ \text{in-kip}/24.375\ \text{in})}x\ 100(\%)=0.55(\%)$$

Based on the roof girder example, design by elastic analysis in Appendix 1.2 has the following limitations:

1) The calculation of the proper effective unbraced length under partial bracing is illusive, since the unbraced length of a member in Appendix 1.2 is typically calculated assuming full bracing.
2) The appropriateness of a 0.8 stiffness reduction for beam LTB, or more generally, the appropriateness of using a higher margin of safety for slender columns in the specifications, but not for slender beam, may be called into question.
3) The sufficiency of a cross-section resistance check, combined with the 0.8 stiffness reduction, in representing the substantial loss of flange lateral bending stiffness when the major-axis bending moment approaches and exceeds the cross-section yield moment may be called into question.
4) The above analysis model is extremely complex.

The above limitations preclude the use of the new AISC (2016) Appendix 1, Section 1.2 approach of Design by Elastic Advanced Analysis, since the Appendix 1, Section 1.2 provisions are based effectively on the assumption of full bracing in the calculation of $\phi_b M_n$. Furthermore, elastic analysis models are not applicable in general to assess the strength of members restrained by flexible elastic bracing systems.

5. Assessment by AISC (2016) Appendix 1, Section 1.3 (Design by Inelastic Analysis)

For the design assessment using Appendix 1.3, a full nonlinear analysis is conducted directly modelling member and frame imperfections. In this approach, the assessment of the available strength of the members and is addressed directly by the analysis.

In applying Appendix 1.3, the analysis is performed including the following required considerations:

1) All loads corresponding to LRFD load combination.

2) Torsional member deformations.
3) Geometric nonlinearities including both *P-Δ* and *P-δ* effects and twisting effects. The use of approximate methods appearing in Appendix 8 is not permitted.
4) In all cases, directly modelling initial imperfections, such as initial out-of-straightness (L_b/1000 or L_b/2000) for member and initial out-of-alignment (L_b/500) for frame. The pattern of the initial imperfections shall be taken considering the greatest destabilizing effect for the load combination being considered. The use of notional loads to represent is not permitted.
5) Stiffness reduction using 0.9 times the nominal elastic stiffnesses.
6) Use of a factored yield strength of 0.9 times the specified minimum yield strength, F_y.
7) Direct modeling of residual stresses.

To evaluate required strength and bracing stiffness by the Appendix 1.3, the roof girder is modeled using ABAQUS shell FEA model. This has the following characteristics:

- The roof girder in Fig.1 is modeled using shell element. Both flanges 12 elements and web 16 elements in each cross-section.
- The Best-Fit Prawel residual stress in Fig.7 are employed for the welded cross-section.

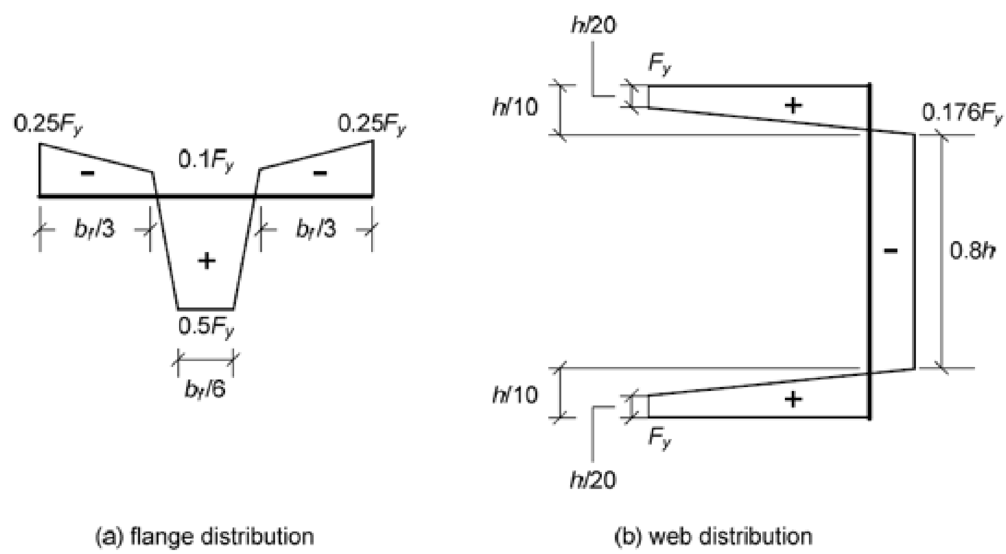

Figure 7. Best-Fit Prawel residual stress.

- Shear panels are modeled at the top flange between the purlin having 5 ft spacing using a spring model that resists the relative movement between the braced points in the direction of the bracing. Torsional braces are modeled similarly, using a relative spring model between the top and bottom flanges of the roof girder at the mid-span and at 10 and 20 ft from the mid-span as shown in Fig.1. For the bracing stiffnesses, two reduction factors, $\phi = 0.9$ per AISC Appendix 1.3 and $\phi = 0.75$ per Appendix 6 are considered and the calculated bracing stiffnesses are :

- Reduced shear panel stiffnesse per Appendix 1.3: $\phi\beta_{br} = 0.9x5\,\frac{\text{kip}}{\text{in}} = 4.5\,\frac{\text{kip}}{\text{in}}$
- Reduced shear panel stiffnesses per Appendix 6: $\phi\beta_{br} = 0.75x5\,\frac{\text{kip}}{\text{in}} = 3.75\,\frac{\text{kip}}{\text{in}}$
- Reduced torsional bracing stiffness per Appendix 1.3:
  $$\phi\frac{\beta_T}{h^2} = 0.9x\frac{6400\text{in-kip/rad}}{(24.375\text{in})^2} = 9.694\,\frac{\text{kip}}{\text{in}}$$
- Reduced torsional bracing stiffness per Appendix 6:
  $$\phi\frac{\beta_T}{h^2} = 0.75x\frac{6400\text{in-kip/rad}}{(24.375\text{in})^2} = 8.078\,\frac{\text{kip}}{\text{in}}$$

- At each purlin location, gravity load -3.7796 kip is applied and at each end 20kip compressive axial load and 2724 in-kip moment are applied.
- The left-hand end of the roof girder is constrained against the three translational displacements in the X, Y and Z direction. The right-hand end of the roof girder is constrained against the two translational displacements in the Y and Z direction.
- Twist rotation of the girder is rigidly constrained at both of its ends.
- Initial geometric imperfections are directly modeled in the girder top flange in the unbraced lengths adjacent to the mid-span using Fig.3 and Fig.4 at the mid-span. The two out-of-straightness values (L_b/1000 and L_b/2000) and the out-of-alignment of the relevant braced points of L_b/500 are employed.
- The 0.9 reduction factor is applied to the elastic modulus and to the yield strength, which are thus 0.9E=0.9x29,000ksi=26,100ksi and 0.9Fy=0.9x50ksi = 45 ksi.

Figure 8 shows the failure mode of the roof girder using 0.9 stiffness reduction and initial geometric imperfection L_b/2000 and L_b/500 and one-half of the Best-Fit Prawel residual stresses. The failure mode of the roof girder in Fig.8 is consistent with the buckling mode using SABRE2 (White et al. 2016) (shown subsequently).

Figure 8. Failure mode per AISC (2016) Appendix 1.3 solution.

In Fig.9, the relationship between the torsional bracing force and Applied Load Ratio (APR) with respect to initial geometric imperfection and residual stress is evaluated. In Fig.9, the maximum APR using out-of-straightness L_b/1000 and full Best-Fit Prawel residual stress is 0.85. The bracing force at the maximum APR is 0.46% of the design bracing force. The maximum APR using out-of-straightness *Lb*/2000 and half Best-Fit Prawel residual stress is 0.91. The bracing force at the maximum APR is still 0.46% of the design bracing force. The torsional bracing force is not influenced by the initial imperfection and residual.

In Fig.10, the relationship between the torsional bracing force and APR with respect to $\phi = 0.75$ and $\phi = 0.9$. The roof girder is modeled using out-of-straightness *Lb*/2000 and half Best-Fit Prawel residual stress. The torsional brace force of $\phi = 0.9$ at maximum APR is 0.46%. In addition, the torsional brace force of $\phi = 0.75$ at maximum APR is 0.46% of design brace force.

In Fig.11, the relationship between the shear panel bracing force and Applied Load Ratio(APR) (i.e., the applied fraction of the required design load) is shown using out-of-straightness L_b/2000 and one-half of the Best-Fit Prawel residual stresses. The available design strength of the roof girder is 0.91 of the required design load. That is, the limit load of the system is attained at an APR of 0.91. The shear panel bracing force at this APR is 0.53% of the girder flange force at the braced location.

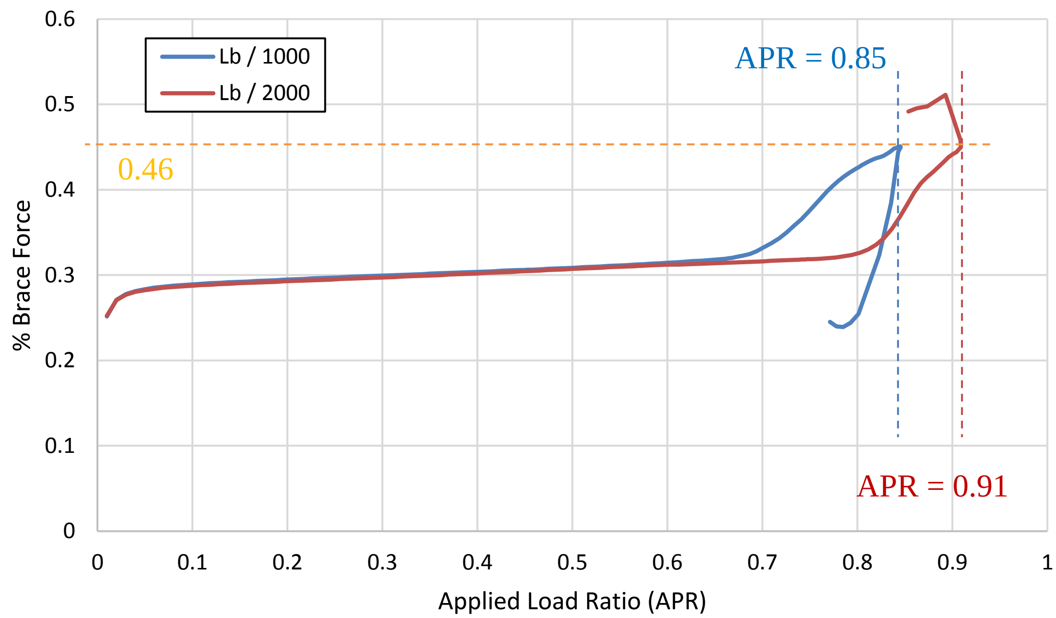

Figure 9. Torsional brace force vs Applied Load Ratio (APR) with respect to the combination of out-of-straightness and Best-Fit Prawel residual stresses.

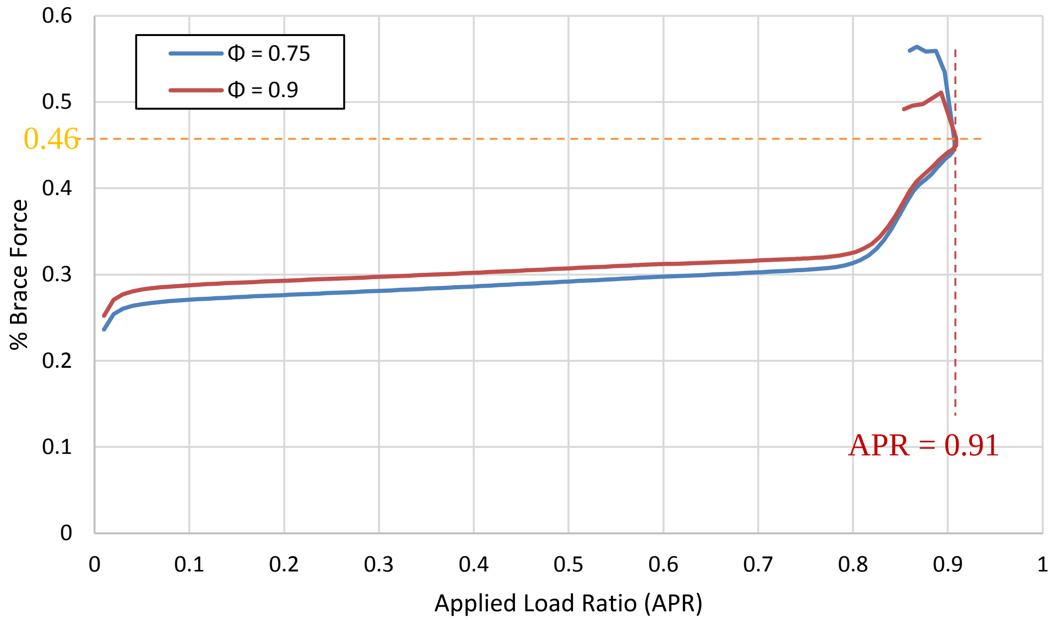

Figure 10. Torsional brace force vs Applied Load Ratio with respect to the bracing stiffness reduction factor.

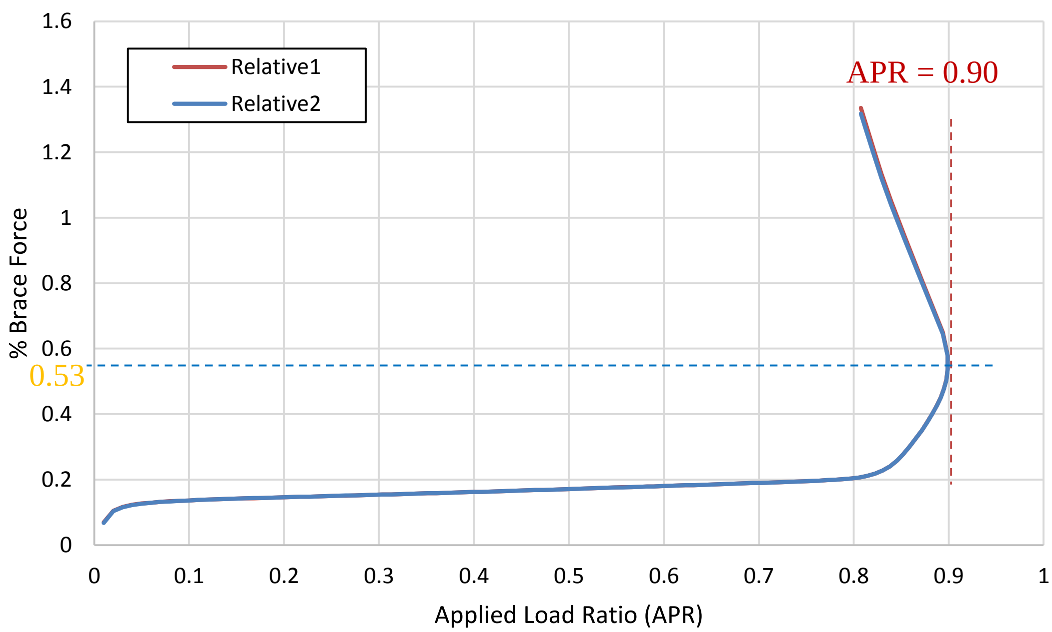

Figure 11. Shear panel brace force vs the Applied Load Ratio.

6. Assessment by Inelastic Buckling Analysis

This section presents a comprehensive approach for the design of structural steel members and systems via the use of buckling analysis combined with appropriate column, beam and beam-column inelastic stiffness reduction factors. The stiffness reduction factors are derived from the ANSI/AISC 360 Specification column, beam and beam-column strength provisions. The resulting procedure provides a rigorous check of member design resistances accounting for continuity effects across braced points, as well as lateral and/or rotational restraint from other framing including a wide range of types and configurations of stability bracing. No separate checking of the corresponding underlying Specification member design resistance equations is required. In addition, no calculation of design strength factors, such as effective length (K) factors and moment gradient and/or load height (C_b) factors, is necessary. The buckling analysis model directly captures the fundamental mechanical responses associated with the design strength factors. For the design of beam-columns and frames, the approach may be used with the AISC Direct Analysis Method (the DM) or the Effective Length Method (the ELM). The DM or ELM requirements are satisfied in the second-order elastic analysis calculation of the required member strengths (i.e., the internal member forces), accounting for pre-buckling load-displacement effects. The buckling analysis captures the member design resistances. This approach provides a particularly powerful mechanism for the design of frames utilizing general stepped and/or tapered I-section members. Two inelastic buckling analysis are available and given by:

1) Inelastic Linear Buckling Analysis (ILBA) – buckling of the elastic or inelastic structure neglecting the influence of pre-buckling displacements. To obtain the inelastic buckling load, SABRE2 (White et al. 2016) uses an extension and generalization of the traditional AISC column inelastic Stiffness Reduction Factor (SRF) method. This approach provides for the calculation of the buckling resistance of any type of I-section column, beam or beam-column member. The SABRE2 inelastic buckling algorithm can be used to produce a rigorous direct calculation of the AISC member axial resistance, $\phi_c P_n$, the AISC member flexural resistance, $\phi_b M_n$, and/or the AISC-based beam-column resistance under combined axial compression (or tension) and flexure. SABRE2 can account for the influence of any type or combination of bracing, member end translational, rotational and/or warping restraint, and continuity with adjacent framing within its calculation of the inelastic buckling resistance.

2) Inelastic Nonlinear Buckling Analysis (INBA) – buckling of the elastic or inelastic structure considering pre-buckling displacement effects. For beam-type members, inelastic linear buckling analysis usually is sufficient to determine the flexural resistance $\phi_b M_n$. In addition, column axial resistances, $\phi_c P_n$, can be obtained sufficiently from an inelastic linear buckling analysis in problems where the pre-buckling flexural and torsional displacements are relatively small. However, for general members and frames, the solution must track the changes in the structure's geometry under the applied load to satisfy the AISC design requirement that equilibrium must be considered on the deflected geometry of the structure. The SABRE2 INBA algorithm calculates the pre-buckling load-deflection response based on either the AISC Effective Length or Direct Analysis method rules. However, SABRE2 replaces the traditional checks of the member resistances via Specification algebraic resistance equations, which use various approximations such as C_b, K_x, K_y, K_z, etc., by the direct calculation of the buckling resistance of the structure with its members having reduced stiffnesses derived from the Specification resistance equations. As a result, SABRE2 provides a rigorous calculation of $\phi_c P_n$, $\phi_b M_n$, and/or the beam-column resistances within the context of the AISC Effective Length or Direct Analysis methods. The need to determine resistances from the AISC Specification strength equations is replaced by a more general buckling analysis calculation. This allows for a more accurate implementation of the Specification provisions.

Inelastic Nonlinear Buckling Analysis (INBA) as implemented in SABRE2, which is derived from and expands the AISC (2016) Chapter C, E, F and H and Appendix 6 provisions to allow for the overall assessment of the roof girder strength and the adequacy of the stiffness of the bracing system, combined with simple member force percentage rules from Appendix 6 for the assessment of the bracing system strength requirements. The phrase "(Current Strength Eqs.)" indicates that the solution is based on the current beam, column and beam-column equations in the AISC 360-16 Specification. Under *Analysis Parameters*, the program also provides a solution option that is based on recommended modifications that provide an improved characterization of member strengths (Subramanian 2015).

Figure 12 shows the governing overall lateral-torsional buckling (LTB) mode for the above roof girder, determined using the INBA algorithm in SABRE2. The lines shown with a diamond symbol in the horizontal plan at the top flange level represent the shear panel bracing from the roof deck, and the circular lines at the mid-span and at the two locations on each side of the mid-span, denote the torsional bracing from the roof purlins and the framing of a flange diagonal to the bottom flange of the girder. The magenta arrow symbols indicate zero displacement constraints, and the green arrows represent the applied loads.

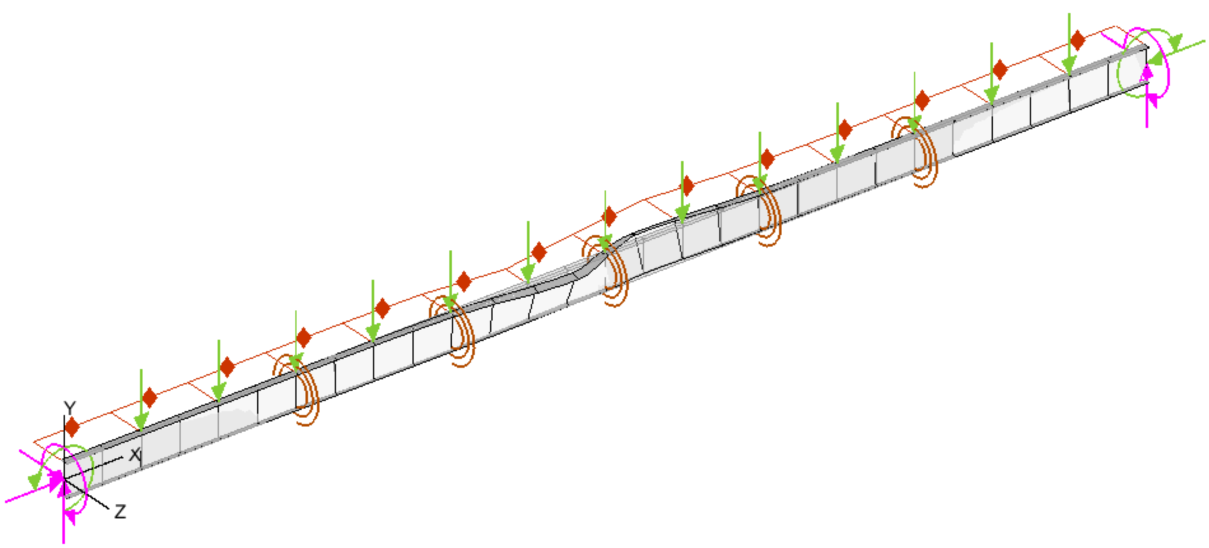

Figure 12. Governing overall lateral-torsional buckling mode for the roof girder using Inelastic nonlinear buckling analysis from SABRE2 (White et al. 2016).

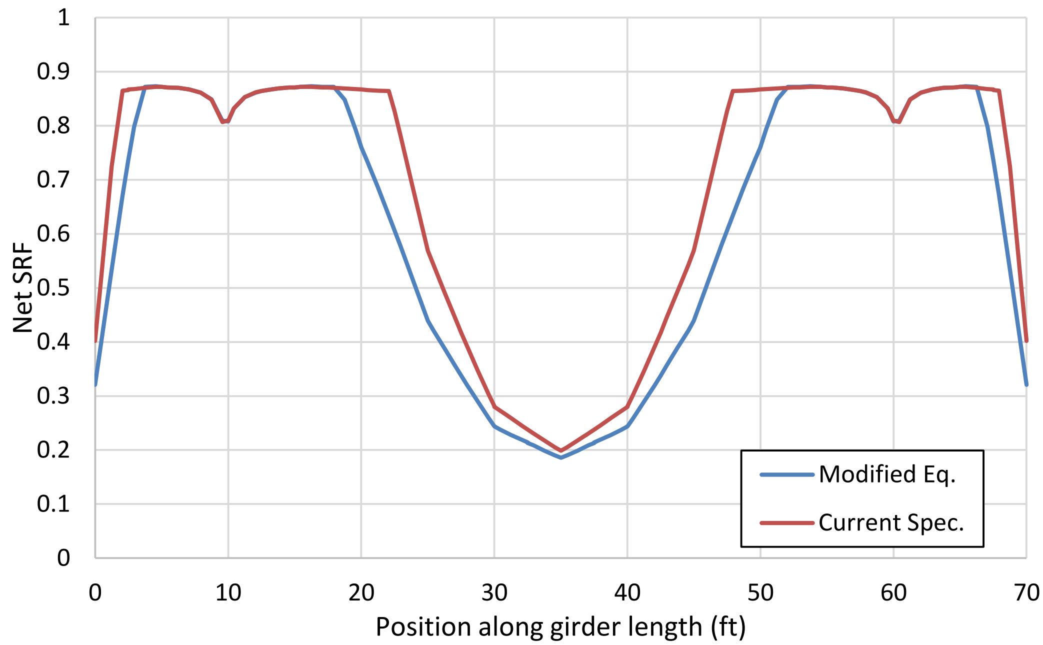

Figure 13. Variation of the net Stiffness Reduction Factor (SRF) along the length of the roof girder at its maximum design resistance corresponding to γ_n = 0.92058 (current AISC Specification) and γ_n = 0.85852 (modified resistance equation).

The applied load ratio at incipient inelastic buckling of the roof girder under the required gravity load is γ_n = 0.92058 (current resistance equation) and γ_n = 0.85852 (modified resistance equation). Therefore, the girder and its bracing system are not quite sufficient to support the required LRFD loading. It should be noted that if the axial load is assumed to be zero, a γ_n of 1.0096 is obtained from an ILBA, indicating that the roof girder and its bracing system are sufficient to support the required loading neglecting the axial loading effects. A γ_n of 1.0101 is obtained from an INBA, illustrating the fact that pre-buckling displacement effects are negligible for in this problem when only considering the flexural loading. A γ_n of 0.97294 is obtained from an ILBA with the required axial loading included, showing that there is a minor second-order effect of the axial load acting through the girder vertical displacements in the plane of the web in this problem.

One can observe a noticeable lateral deflection within the adjacent shear panels on each side of the mid-span torsional brace in Fig. 12. This indicates that the light roof panel bracing is indeed providing less than full bracing at the first braced point on each side of the mid-span (based on the idealization of the bracing stiffness as the nominal stiffness divided by $2/\phi$). Nevertheless, the overall design strength is slightly larger than the LRFD required strength if the axial loading is neglected. Figure 13 shows that significant yielding is developed both at the mid-span and at the girder ends when the system maximum design resistance is reached. Also, there is a slight decrease in the net SRF in the vicinity of the girder inflection points. This decrease is due to the use of a net SRF equal to 0.9 x 0.877 x τ_a at locations where the moment approaches zero, where τ_a is the traditional AISC column stiffness reduction factor, whereas at locations dominated by bending actions, the net SRF approaches 0.9 x τ_{ltb}, where τ_{ltb} is a basic stiffness reduction factor derived from the AISC (2016) lateral torsional buckling resistance equations. The development of stiffness reduction factors that match rigorously with the AISC (2016) resistance equations is discussed in detail by White et al. (2015).

It is important to emphasize that the accurate assessment of the combined bracing stiffnesses is somewhat challenging for this problem using any method other than the SABRE2 buckling analysis. The basic requirements specified in AISC Appendix 6 do not address combined lateral and torsional partial bracing.

The AISC (2016) Appendix 1 provisions provide guidance for the use of advanced load-deflection analysis methods for general stability design. However, the application of these methods necessitates the modeling of an appropriate initial out-of-alignment of the girder braced points as well as out-of-straightness of the girder flanges between the braced points. The geometric imperfections needed to evaluate the different bracing components are in general different for each of the bracing components, and the geometric imperfections necessary to evaluate the maximum strength of the girder are in general different from those necessary to evaluate the bracing components. One can rule out the need to perform many of these analyses by identifying the girder critical unbraced lengths as well as the critical bracing components. However, short of the type of buckling analysis provided by SABRE2, it can be difficult to assess which unbraced lengths and which bracing components are indeed the critical ones. SABRE2 provides not only an assessment of the adequacy of the bracing system stiffnesses, but it also provides a "direct" check of the member design resistance given the member's bracing restraints and end boundary conditions.

The only shortcoming of the above buckling analysis approach in the context of the above type of design problem is that this approach does not provide any direct estimate of the bracing strength requirements. However, based on numerous results from experimental testing and from refined FEA simulation of experimental tests, it is recommended that the simple member force percentage rules of AISC (2016) Appendix 6 can be used to specify the minimum required strengths for the different bracing components.

Advantages of inelastic buckling analysis approach are:

- More general and more rigorous handling of all types of bracing, end restraint and continuity effects
- No need for separate column and beam buckling analysis or K factor calculations (along with the corresponding anomalies & paradoxes), followed by mapping to column & beam strength curves, followed by plugging everything into a simplified beam-column strength interaction curve
- Substantially cleaner, more streamlined and less error prone member strength calculations.
- Consistent bracing stiffness an member strength assessments
- More accurate capture of moment gradient effects plus tapered and stepped member geometry effects via a continuous representation of the corresponding τ values along the member lengths
- More accurate strength check under general loading including load height

Design assessment via rigorous test simulation procedures, which is permitted by AISC (2016) Appendix 1, Section 1.3. This approach provides for a direct calculation of the bracing system strength requirements, in addition to checking of the adequacy of the bracing system stiffnesses. However, the amount of labor associated with defining appropriate geometric imperfections for this direct assessment is prohibitive for routine design, unless all of this labor can be automated within software in some fashion. Furthermore, the computational demands are much greater compared to the approach in SABRE2 (White et al. 2016).

7. Conclusion

This paper assesses various methods to calculate required design strength of a general roof girder design problem and evaluates the strengths and limitations in each method. In practical design, partial and full bracing, continuity, various boundary conditions, general loading including moment gradient load and load height may need to be considered. The DM and the ELM do not generally provide the capability for rigorous calculation of the required strength for some of these general conditions. The design strength check using AISC Appendix 1.2 is also difficulty due to the selection of unbraced length of the member or frame including partial bracing. Furthermore, the implementation of Appendix 1.2 generally requires relatively complex modeling of geometric imperfections. Inelastic buckling analysis provides the required design strength including general bracing and general loads and easy to model. The calculation of the required design strength including general bracing and general loads is available using AISC Appendix 1.3. However, this method requires substantial effort compared to the use of the inelastic buckling analysis method.

References

AISC (2015), "Specification for Structural Steel Buildings," Draft AISC 360 Specification 2016, Ballot 4, August.

AISC (2015). "Specification for Structural Steel Buildings," ANSI/AISC 360-10, American Institute of Steel Construction, Chicago, IL.

AISC (2002). "Example Problems Illustrating the Use of the New Bracing Provisions – Section C3, Spec and Commentary," Ad hoc Committee on Stability Bracing, November.

ASCE (1997). *Effective Length and Notional Load Approaches for Assessing Frame Stability: Implications for American Steel Design*, American Society of Civil Engineers, Reston, VA.

Lokhande, A.M. and White, D.W. (2014). "Evaluation of Steel I-Section Beam and Beam - Column Bracing Requirements by Test Simulation," Research Report to the American Institute of Steel Construction. School of Civil and Environmental Engineering, Georgia Institute of Technology, Atlanta, GA.

Prado, E.P. and White D.W. (2014). "Assessment of Basic Steel I-Section Beam Bracing Requirements by Test Simulation," Research Report to the American Institute of Steel Construction, School of Civil and Environmental Engineering, Georgia Institute of Technology, Atlanta, GA.

Jeong, W.Y. (2014). "Structural Analysis and Optimized Design of General Nonprismatic I-Section Members," Doctoral Dissertation, School of Civil and Environmental Engineering, Georgia Institute of Technology, Atlanta, GA.

Subramanian, L.P.(2015). "Flexural Resistance of Longitudinally stiffened Plate Girders," Doctoral Dissertation, School of Civil and Environmental Engineering, Georgia Institute of Technology, Atlanta, GA.

Salvadori, M.G. (1955). “Lateral Buckling of Beams,” Transactions ASCE, Vol. 120, 1165.

Oğuzhan Toğay, Woo Yong Jeong, Cliff D. Bishop, and Donald W. White (2015). “Toward a More Comprehensive Approach for Design using Buckling Analysis,” Proceedings of the Annual Stability Conference, SSRC, Nashville, TN, March 25-27.

White, D.W., Jeong, W.Y. and Toğay, O. (2015). “Comprehensive Stability Design of Steel Members and Systems via Inelastic Buckling Analysis,” Keynote paper of 8th International Symposium on Steel Structures, Jeju, South Korea, November 5-7.

White, D.W., Jeong, W.Y. and Toğay, O. (2016). “SABRE 2,” < white.ce.gatech.edu/sabre > (Jan. 20, 2016).

Yura, J.A., Galambos, T.V. and Ravindra, M.K. (1978). “The Bending Resistance of Steel Beams,” Journal of the Structural Division, ASCE, 104(ST9), 1355-1370.

Yura, J.A. (2001). “Fundamentals of Beam Bracing,” Engineering Journal, AISC, 38(1), 11-26.

Ziemian, R.D. (2014). “MASTAN2 v3.3,” <www.mastan2.com> (Jan 17, 2015).